32nd URSI GASS, Montreal, 19-26 August 2017

Satellite-beacon Ionospheric-scintillation Global Model of the upper Atmosphere (SIGMA): Enhancements and GPS Signal Propagation Modeling

James P. Conroy (1) and Kshitija Deshpande (2)
(1) Bradley Department of Electrical and Computer Engineering, Virginia Tech, Blacksburg, Virginia, USA, 24061, osujim1@vt.edu
(2) Department of Physical Sciences, Embry-Riddle Aeronautical University, Daytona Beach, Florida, USA, 32114

Abstract

In this paper, we present enhancements made to the spectral modeling capabilities of the previously developed SIGMA for Ionospheric propagation. The incorporation of Shkarofsky's generalized spectrum offers the flexibility required to more effectively represent the wide range of electron density distributions observed in Equatorial and Polar Regions. In exercising this new capability we demonstrate the potential impact that the satellite line-of-sight (LOS), irregularity orientation and degree of anisotropy can have on correlation processing of a received GPS signal. The results from this study provide valuable physical insights into Ionospheric propagation which will aid in further validation of SIGMA as an Ionospheric propagation model.

1. Introduction and Background

Signals which propagate through the Ionosphere are vulnerable to signal degradation due to irregularities in the background electron density [1]. Radio wave scintillation, which is the temporal fluctuation in amplitude and phase of a signal, can result in severe channel fading and random phase variations that can interfere with the performance of a radar, communication or GPS system [2]. It is well known that Ionospheric scintillation has unique characteristics in the Equatorial and Polar Regions resulting from the different spatial distribution of the electron densities [3, 4]. These differences are reflected in the temporal power spectra and signal statistics measured on the ground. While various models have been developed for equatorial use [5], where the electron density tends to be isotropically distributed, and efforts have been made to extend simulations to high-latitude regions [6], there is still a need to develop modeling capabilities which can more effectively represent the anisotropic electron density distributions in these regions. This paper summarizes the recent enhancements made to the previously developed SIGMA Ionospheric propagation model [6]. The enhancements, which include incorporating Shkarofsky's generalized turbulence spectrum [7, 8], offers increased flexibility for modeling the wide range of electron density distributions observed across all regions of the earth. This new version of SIGMA is then used to investigate the impact of satellite line-of-sight (LOS), plasma drift velocity, and the degree of electron density anisotropy on the performance of GPS correlation processing. The results from this study provide first-order physical insights into Ionospheric propagation which could potentially aid in future model validation efforts.

2. Model

SIGMA is a full three dimensional (3D) electromagnetic (EM) wave propagation model developed by [6], which simulates signal propagation through Ionospheric irregularities. In order to perform a simulation, SIGMA requires inputs which describe the structure and motion of the irregularities as well as geographical and propagation information. These inputs are used to produce realizations of the Ionospheric electron density structure whose impact on wave propagation is analyzed using a set of diffractive phase screens aligned with the local magnetic field [9, 10].

2.1 Input Parameters

A set of SIGMA simulations were completed using the inputs from [6] as the starting point in order to establish a baseline. A transmit frequency of 1575.42 MHz (L1) was used for a receiver located at 74.4° N (latitude) and 264.9° E (longitude). This location was selected in order to simulate data as if it were acquired by the scintillation receiver at the Resolute Bay station of the Canadian High Arctic Ionospheric Network (CHAIN) [9] which has a magnetic field inclination of 87.6°. The Ionosphere was modeled as a single layer by assuming weak scattering. The thickness of the layer was 10 Km, the width was 50 Km, and the altitude to the top of the layer was 120 Km. The magnitude of the plasma drift velocity vector, which was directed along the x or y axis (Figure 1), was 500 m/s. Four different stationary transmit satellite locations, including $[\theta,\phi]$ values of $[0^{\circ},0^{\circ}]$, $[45^{\circ},0^{\circ}]$, $[45^{\circ},45^{\circ}]$, and $[45^{\circ},90^{\circ}]$, were evaluated for simplicity. The outer scale of the plasma irregularities was set to 2 Km, the standard deviation of background electron density 2E11 (m^{-3}) and the 3D spectral index was 3. The axial ratio, which is a parameter that defines the anisotropy of the irregularities, was varied using scaling factors α_x, α_y, and

α_z, and then applied in the spectral model to specify the spectral shape.

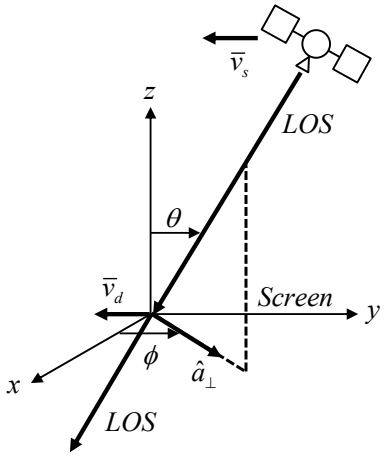

Figure 1. Geometry of the setup used in SIGMA. Modified from [6].

The simulations included in this paper were completed with α_x values of 3 and 10 and $\alpha_{y,z}$ equal to unity. The scaling values and velocity vectors were chosen in order to compare the effect of elongated versus short irregularities (Figure 2) with relatively simple plasma motion and satellite geometry combinations. These input parameters were used to produce scintillation sequences 30 second in duration with a sampling rate of 50 Hz.

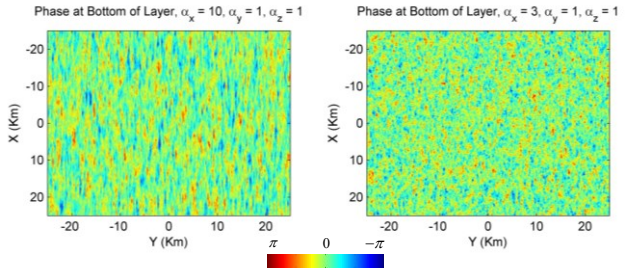

Figure 2. Phase at the bottom of irregularity layer for αx=10 (left) and αx=3 (right).

2.2 Spectrum

The Shkarofsky spectrum used to simulate the electron density structure is given by:

$$\Phi_\xi(\mathbf{k}) = \frac{\sigma_N^2 (k_0 r_0)^{(p-3)/2} r_0^3}{(2\pi)^{3/2} K_{(p-3)/2}(k_0 r_0)} \times \left(r_0\sqrt{k^2+k_0^2}\right)^{-p/2} \times K_{(p/2)}\left(r_0\sqrt{k^2+k_0^2}\right) \quad (1).$$

In order to evaluate (1), it is required that $k_0 r_0 \ll$ to effectively approximate the Hankel functions (given here as K). An inner scale value of r_0 of 0.01 m was used for this purpose. The scaling factors α_x, α_y and α_z were applied to (1) by substituting (2) into (1) and then multiplying by $\alpha_x\alpha_y\alpha_z$.

$$k^2 = \alpha_x^2 k_x^2 + \alpha_y^2 k_y^2 + \alpha_z^2 k_z^2 \quad (2).$$

2.3 GPS Signal Model

The GPS signal model with scintillation amplitude $\varepsilon(t)$ and phase errors $\psi(t)$ is included in (3), where P_C is the carrier power, $C(t)$ is the gold code sequence and $D(t)$ are the navigation data bits. For this study, the P_C was defined using typical GPS link parameters including the minimum guaranteed signal strength of -160 dBW, bandwidth of 10 MHz and system noise temperature of 290 K [10].

$$s(t) = (1+\varepsilon(t))\sqrt{2P_C}C(t)D(t)\cos(2\pi ft + \psi(t)) \quad (3).$$

3. Results

The results for α_x equal to 10 and x-directed velocity are included in Figure 3. These results indicate that the correlator outputs within the x-z plane remain largely unperturbed and locked, perhaps due to the very long irregularities which are also oriented along the x axis. In comparison, the correlator outputs for signals received from satellites not contained within the x-z plane show time variations due to the presence of the irregularities and come close to losing lock.

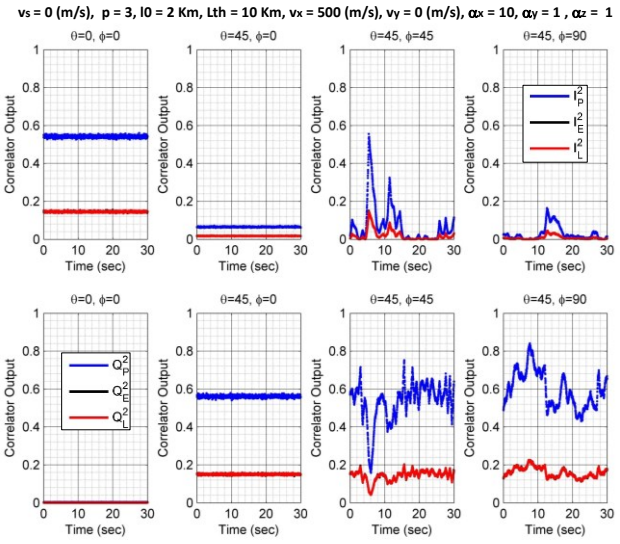

Figure 3. GPS early, prompt and late correlator outputs for vx=500 (m/s), vy=0 (m/s), and αx=10.

The results for α_x equal to 10 and the y-directed velocity are included in Figure 4. These results indicate that the correlator outputs for signals received from all satellites except $[45^\circ, 90^\circ]$ have faster time variations than previously observed while $[45^\circ, 0^\circ]$ and $[45^\circ, 45^\circ]$ come close to losing lock. The fast variation may be due to the higher spatial frequency content of the irregularities.

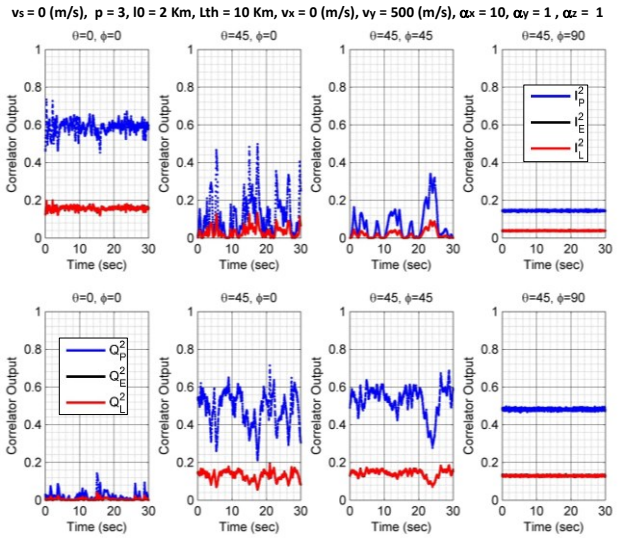

Figure 4. GPS early, prompt and late correlator outputs for vx=0 (m/s), vy=500 (m/s), and αx=10.

The results for α_x equal to 3 and the x-directed velocity are included in Figure 5. These results indicate that as before, the correlator outputs within the x-z plane remain largely unperturbed and well locked. In comparison, the correlator outputs for signals received from satellites not contained within the x-z plane show time variations due to the presence of the irregularities which appear to fluctuate more rapidly than before.

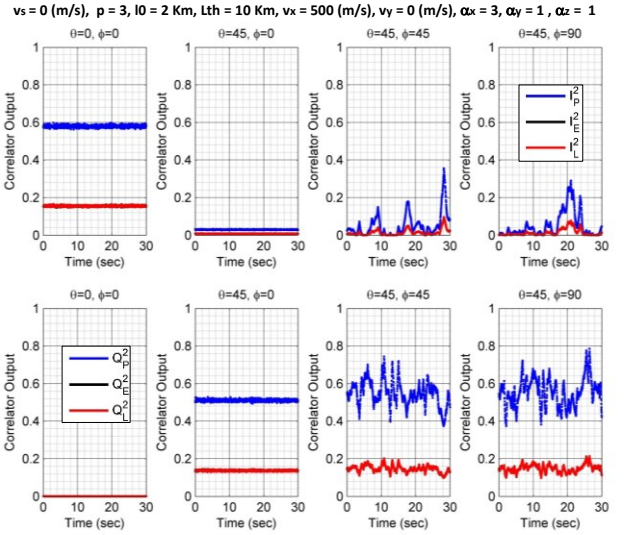

Figure 5. GPS early, prompt and late correlator outputs for vx=500 (m/s), vy=0 (m/s), and αx=3.

The results for α_x equal to 3 and the y-directed velocity are included in Figure 6. These results demonstrate that the outputs within the y-z plane once again easily maintain lock though the signal from the satellite at $[0^\circ, 0^\circ]$ is somewhat perturbed. In comparison, the correlator outputs for satellites not contained within the y-z plane vary relatively fast and come close to losing lock on several occasions.

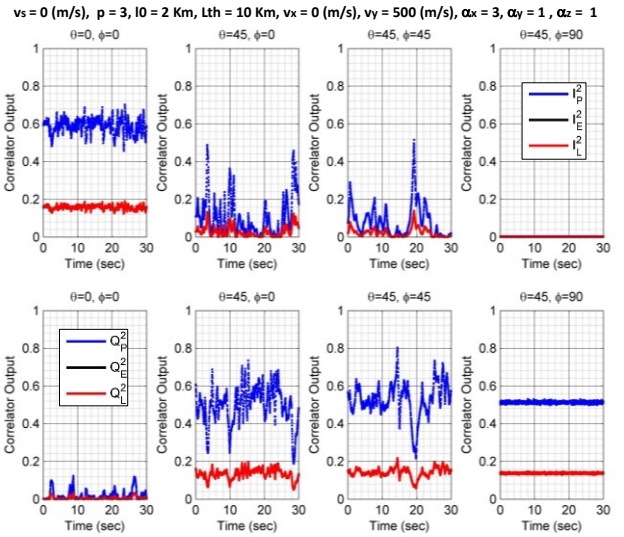

Figure 6. GPS early, prompt and late correlator outputs for vx=0 (m/s), vy=500 (m/s), and αx=3.

4. Conclusions

In this paper, we have presented upgrades made to the spectral modeling capabilities of the previously developed SIGMA which offers increased flexibility for modeling a wide range of electron density distributions. This new

version of SIGMA was then used to demonstrate the potential impact that the satellite line-of-sight, irregularity orientation and degree of anisotropy can have on a received GPS signal. The results from this study provide valuable first-order physical insights into Ionospheric propagation which will potentially aid in future SIGMA validation efforts.

5. Acknowledgements

We would like to Dr. Wayne Scales, Dr. Amir Zaghloul, Dr. Gary Bust and Dr. Michael Kelly for their support. AMDG.

6. References

1. *Ionospheric propagation data and prediction methods required for the design of satellite services and systems*, International Telecommunications Union Recommendation (ITU-R) P.531-12, 2013.

2. Satellite-Based Augmentation Systems Ionospheric Working Group (2012, April). *How Irregularities in Electron Density Perturb Satellite Navigation Systems* [Online]. Available: http://gpsworld.com/

3. J. Aarons, "Global morphology of ionospheric scintillations," in *Proceedings of the IEEE*, vol. 70, no. 4, pp. 360-378, April 1982.doi: 10.1109/PROC.1982.12314

4. S. Basu *et al*., "Characteristics of plasma structuring in the cusp/cleft region at Svalbard," in *Radio Science*, vol. 33, no. 6, pp. 1885-1899, Nov.-Dec. 1998. doi: 10.1029/98RS01597

5. T. E. Humphreys, *et al.,* "Simulating Ionosphere-Induced Scintillation for Testing GPS Receiver Phase Tracking Loops," in *IEEE Journal of Selected Topics in Signal Processing*, vol. 3, no. 4, pp. 707-715, Aug. 2009. doi: 10.1109/JSTSP.2009.2024130

6. K. B. Deshpande, *et al.,* "Satellite-beacon Ionospheric-scintillation Global Model of the upper Atmosphere (SIGMA) I: High latitude sensitivity study of the model parameters," in *Journal of Geophysical Research (Space Physics)*, vol. 119, no. 5, pp. 4026–4043, May, 2014. doi:10.1002/2013JA019699.

7. I. P. Shkarofsky, "Generalized turbulence space-correlation and wave-number spectrum function pairs," in *Canadian Journal of Physics*, vol. 46, no. 19, pp. 2133, 1968. doi:10.1139/p68-562.

8. C. S. Carrano, *et al.,* "Multiple phase screen modeling of ionospheric scintillation along radio occultation raypaths," in *Radio Science*, vol. 46, no. 06, pp. 1-14, Dec. 2011. doi: 10.1029/2010RS004591

9. P. T. Jayachandran *et al*., "Canadian high arctic ionospheric network (CHAIN)," in *Radio Science*, vol. 44, no. 01, pp. 1-10, Feb. 2009.doi: 10.1029/2008RS004046.

10. K. Borre, *et al.,* in *A Software-Defined GPS and Galileo Receiver: A Single-Frequency Approach*, 1st ed., 2007.